Different universality classes of isostructural U*TX* compounds (T = Rh, Co, $Co_{0.98}Ru_{0.02}$; X = Ga, Al)

Petr Opletal, Vladimír Sechovský, and Jan Prokleška
Charles University, Faculty of Mathematics and Physics, Department of Condensed Matter Physics Ke Karlovu 5, Prague 2, Czech Republic

(Received 26 August 2020; revised 16 November 2020; accepted 16 December 2020; published 31 December 2020)

Magnetization isotherms of the 5f-electron ferromagnets URhGa, UCoGa, and $UCo_{0.98}Ru_{0.02}Al$ were measured at temperatures in the vicinity of their Curie temperature to investigate the critical behavior near the ferromagnetic phase transition. These compounds adopt the layered hexagonal ZrNiAl-type structure and exhibit huge uniaxial magnetocrystalline anisotropy. The critical β, γ, and δ exponents were determined by analyzing Arrott-Noakes plots, Kouvel-Fisher plots, critical isotherms, scaling theory, and Widom scaling relations. The values obtained for URhGa and UCoGa can be explained by the results of the renormalization group theory for a two-dimensional (2D) Ising system with long-range interactions similar to URhAl reported by other investigators. On the other hand, the critical exponents determined for $UCo_{0.98}Ru_{0.02}Al$ are characteristic of a three-dimensional (3D) Ising ferromagnet with short-range interactions suggested in previous studies also for the itinerant 5f-electron paramagnet UCoAl situated near a ferromagnetic transition. The change from the 2D to the 3D Ising system is related to the gradual delocalization of 5f electrons in the series of the URhGa, URhAl, and UCoGa to $UCo_{0.98}Ru_{0.02}Al$ and UCoAl compounds and appears close to the strongly itinerant nonmagnetic limit. This indicates possible new phenomena that may be induced by the change of dimensionality in the vicinity of the quantum critical point.

DOI: 10.1103/PhysRevB.102.224438

I. INTRODUCTION

Critical phenomena have been one of the most studied issues of physics since the critical points were discovered by Andrews [1]. The continuous (second-order) phase transition was found in systems like ferromagnets [2] to be connected with unified behavior near and at the critical point which can be described by critical exponents. In the case of ferromagnets, three critical exponents, γ, β, and δ, characterize the behavior near and at the critical point. They can be determined from experimental data using the relations [3]:

$$M_S(T) \sim |t|^{\beta}(T < T_C), \tag{1}$$

$$\chi(T)^{-1} \sim |t|^{-\gamma'}(T < T_C), \quad |t|^{-\gamma}(T > T_C), \tag{2}$$

$$M_s \sim (\mu_0 H)^{1/\delta} \text{ for } T = T_C, \tag{3}$$

where M_S is the spontaneous magnetization, χ is magnetic susceptibility, and H is a magnetic field.

The universal behavior near critical points was described by the renormalization group theory first mentioned by Kadanoff [4] and then fully developed by Wilson [5–7]. The universality class is determined by dimensionality of the system d, dimensionality of the order parameter n, and the range of the interaction. There exist several universality classes in magnetism. The most known are three-dimensional (3D) Ising ($n = 1$), XY model ($n = 2$), and 3D Heisenberg ($n = 3$).

It is desirable to investigate how a certain universal critical behavior and magnetic dimensionality is related to the particularities of a given material (symmetry of crystal structure, hierarchy and anisotropy of magnetic interactions, degree of localization of "magnetic" electrons, etc.). Large groups of isostructural compounds containing transition-element ions with one type of "magnetic" d or f electrons provide useful playgrounds for investigation of these aspects. The U*TX* compounds (T = transition metal, X = p-metal) crystallizing in the hexagonal ZrNiAl-type structure constitute such a suitable group of materials [8]. The crystal structure consists of U-T and T-X basal plane layers alternating along the c axis. The strong bonding of 5f-electron orbitals within the U-T layer in conjunction with strong spin-orbit interaction leads to a huge uniaxial magnetocrystalline anisotropy that locks the U magnetic moments in the c axis and thus makes these materials suitable for investigating Ising systems.

The critical magnetic behavior has so far been studied on two compounds of this isostructural group, UCoAl [9] and URhAl [10]. UCoAl is an itinerant 5f-electron paramagnet undergoing, at low temperatures, a metamagnetic transition with a critical field of ~0.7 T [11]. Karube *et al.* [9] reported that it behaves near the critical endpoint as a 3D Ising system with short-range interactions. On the other hand, URhAl was reported as behaving like a two-dimensional (2D) Ising ferromagnet with long-range interactions [10,12] The observed difference between the magnetic dimensionality of UCoAl and URhAl indicates that the common layered hexagonal crystal structure and uniaxial magnetocrystalline anisotropy shared by all compounds of the U*TX* family (X = Al, Ga, Sn, In) [8,11] is not a sufficient condition for sharing also a common magnetic universality class.

To test this aspect, we prepared single crystals of three hexagonal U*TX* ferromagnets, UCoGa [11,13–15], URhGa [16–18], and $UCo_{0.98}Ru_{0.02}Al$ (a close analog of

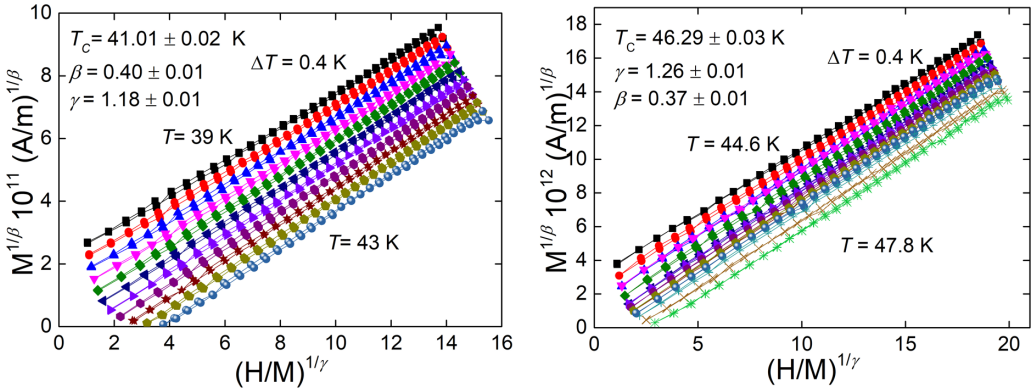

FIG. 1. Modified Arrott plots for URhGa (left) and UCoGa (right). Resulting critical exponents and Curie temperature corresponding to each compound are in the figures. Magnetic curves close to Curie temperature were used for fit of Arrott-Noakes equation.

$UCo_{0.99}Ru_{0.01}Al$ [19,20]), and measured their magnetization isotherms in the neighborhood of their Curie temperature. The measured data were analyzed by investigating Arrott-Noakes plots [21,22], Kouvel-Fischer plots [23], critical isotherms, scaling theory [24], and Widom scaling relations [25] to determine the critical exponents and their corresponding universality classes. The first two compounds were found behaving like 2D Ising systems similar to previously reported URhAl [10], whereas the critical exponents determined for $UCo_{0.98}Ru_{0.02}Al$ point to the 3D Ising universality class similar to UCoAl [9]. Here, we discuss that the change between these two classes of universality is associated with a changing degree of delocalization of $5f$ electrons.

II. EXPERIMENTAL

Single crystals of URhGa, UCoGa, and $UCo_{0.98}Ru_{0.02}Al$ were prepared from stoichiometric melts by the Czochralski method using a triarc furnace. Each single crystal was wrapped in a tantalum foil and sealed in a quartz tube and evacuated to 10^{-6} mbar. The energy-dispersive X-ray (EDX) analysis accomplished with a scanning electron microscope Tescan Mira I LMH equipped by a backscatter electron detector confirmed the stoichiometric composition of URhGa, UCoGa, and $UCo_{0.98}Ru_{0.02}Al$. The x-ray Laue method (Laue diffractometer of Photonic Science) showed good quality of the crystals. Samples for magnetization were cut by a wire saw to a rectangular prism shape [26]. The c-axis magnetization M was measured using an MPMS-7-XL (Quantum Design) in fields from 0.1 to 4 T at different temperatures in the vicinity of Curie temperature.

The values of internal magnetic field H were calculated as:

$$H = H_a - N \times M, \tag{4}$$

where N is the demagnetization factor. The demagnetization factor was evaluated using the formula published by Aharoni [26].

III. RESULTS AND DISCUSSION

A. URhGa and UCoGa

The Curie temperature of a ferromagnet is usually determined by Arrott plot (M^2 vs H/M plot) analysis of magnetization isotherms [21] measured at temperatures in the critical region. The linear Arrott plots are in fact a graphical representation of the Landau equation of state in the theory of second-order phase transition [27–29], which was specified for ferromagnets by Ginsburg [30]. This approach is certainly suitable for investigation of homogenous isotropic ferromagnets. This condition is not met for most real systems, which is documented by considerable curvature in Arrott plots. The value of Curie temperature T_C can be refined by finding the β and γ coefficients for which modified Arrott plots (Arrott-Noakes plots) $M^{1/\beta}$ vs $H/M^{1/\gamma}$ are linear [21]. The Arrott-Noakes plot comes from the analysis of magnetization curves based on the Arrott-Noakes equation [22]:

$$(H/M)^{1/\gamma} = \frac{(T - T_C)}{T_1} + (M/M_1)^{1/\beta}, \tag{5}$$

where M_1 and T_1 are material constants that are temperature independent in the vicinity of the phase transition. Magnetization curves are then fitted by Eq. (5) to get the $M^{1/\beta}$ vs $H/M^{1/\gamma}$ plots linear and parallel by varying free parameters β and γ while keeping the T_1 and M_1 values fixed. The results for our studied compounds are presented in Fig. 1 and Table I together with the best values of T_C and critical exponents β, γ [25].

The critical exponent δ can be calculated from β and γ from the Widom scaling law [25]. It can be determined from the magnetization curve using Eq. (3), too. In Fig. 2, we display the magnetization curves of both compounds in a log-log plot because only the isotherm at T_C is linear in this representation, as seen from Eq. (3). A linear function is then fitted to data points forming the straightest isotherm. The resulting δ values are shown in Fig. 2 and Table I. For URhGa and UCoGa, the δ values calculated from the Widom scaling law [25] are 3.95 and 4.4, respectively, which are close enough to the values of 3.89 and 4.5 shown in Fig. 2. The agreement between values from the Widom scaling law and values from critical isotherms could be improved since we did not know the exact T_C during measurement, and therefore we used isotherms at the temperature closest to the assumed T_C.

The β and γ values can be further refined by analyzing Kouvel-Fisher plots [23], which are based on the definition of critical exponents in Eqs. (1) and (2). The spontaneous

TABLE I. Critical exponents and other relevant parameters obtained for URhGa, UCoGa, and $UCo_{0.98}Ru_{0.02}Al$ by the analysis of Arrott-Noakes plots (A-N plots), Kouvel-Fisher plots (K-F plots), scaling relations (Scaling), critical isotherms (Critical i.), and data for UCoAl [9] for comparison.

	Method	T_C (K)	β	$\gamma'(T < T_C)\gamma(T > T_C)$	δ	σ
URhGa	A-N plots	41.01 ± 0.02	0.40 ± 0.01	1.18 ± 0.01		
	K-F plots	40.91 ± 0.04	0.42 ± 0.02	1.21 ± 0.01		
	Scaling	40.85 ± 0.02	0.39 ± 0.01	1.18 ± 0.01		
				1.19 ± 0.02		
	Critical i.				3.89 ± 0.01	
LR exchange: $J(r) \sim r^{-(d+\sigma)}$, $d = 2$, $n = 1$			0.39	1.18	4.03	1.21
UCoGa	A-N plots	46.29 ± 0.03	0.37 ± 0.01	1.26 ± 0.01		
	K-F plot	46.38 ± 0.06	0.40 ± 0.02	1.29 ± 0.07		
	Scaling	46.23 ± 0.04	0.37 ± 0.01	1.28 ± 0.03		
				1.26 ± 0.02		
	Critical i.				4.32 ± 0.01	
LR exchange: $J(r) \sim r^{-(d+\sigma)}$, $d = 2$, $n = 1$			0.36	1.26	4.5	1.28
$UCo_{0.98}Ru_{0.02}Al$	A-N plots	22.79 ± 0.03	0.32 ± 0.01	1.27 ± 0.01		
	K-F plots	22.79 ± 0.02	0.33 ± 0.01	1.24 ± 0.04		
	Scaling	22.74 ± 0.02	0.325	1.241		
	Critical i.				4.92 ± 0.01	
UCoAl	NMR meas.	–	0.26	1.2	5.4	

magnetization M_S is determined from the intersection of the $M^{1/\beta}$ axis of a Arrott-Noakes plot with straight lines, and the inverse susceptibility χ^{-1} is determined from the intersections of straight lines with the $(H/M)^{1/\gamma}$ axis of the Arrott-Noakes plot. Kouvel and Fisher [23] showed that, by dividing by temperature derivatives of Eqs. (3) and (4), one gets a new set of equations:

$$M_S(T)[dM_S(T)/dT]^{-1} = |T - T_C|/\beta(T), \tag{6}$$

$$\chi^{-1}(T)[d\chi^{-1}(T)/dT]^{-1} = |T - T_C|/\gamma(T). \tag{7}$$

In the vicinity of T_C, the $\beta(T)$ and $\gamma(T)$ became equal to the corresponding critical β and γ values. The critical exponents are determined from the slope, and the Curie temperature is determined from the intersection with the T axis in the Kouvel-Fisher plots shown in Fig. 3. The resulting critical exponents for URhGa and UCoGa are presented in Fig. 3 and Table I.

To check whether the critical exponents above and below the phase transition are equal, we have separately determined the critical exponent $\gamma(T > T_C)$ and γ' $(T < T_C)$ using the scaling theory that predicts a reduced equation of state close to the phase transition [24]:

$$M(\mu_0 H, t) = |t|^{\beta} f_{\pm}(\mu_0 H/|t|^{\beta+\gamma}), \tag{8}$$

where f_+ is for $T > T_C$ and f_- is for $T < T_C$, and both are regular analytical functions. If the correct β, γ, and T_C values are chosen, then the data points in the plot $M(\mu_0 H, t)/|t|^{\beta}$ vs $\mu_0 H/|t|^{\beta+\gamma}$ should fall on two universal curves, one for $T < T_C$ and the second for $T > T_C$, and these curves should approach each other asymptotically. Magnetization data for both compounds were fitted by Eq. (8). The results are shown in Fig. 4 together with the values of critical exponents and T_C, respectively. For both compounds, the difference of the determined critical exponent γ for T above and below T_C is very small, which corroborates the presumption that it does not change.

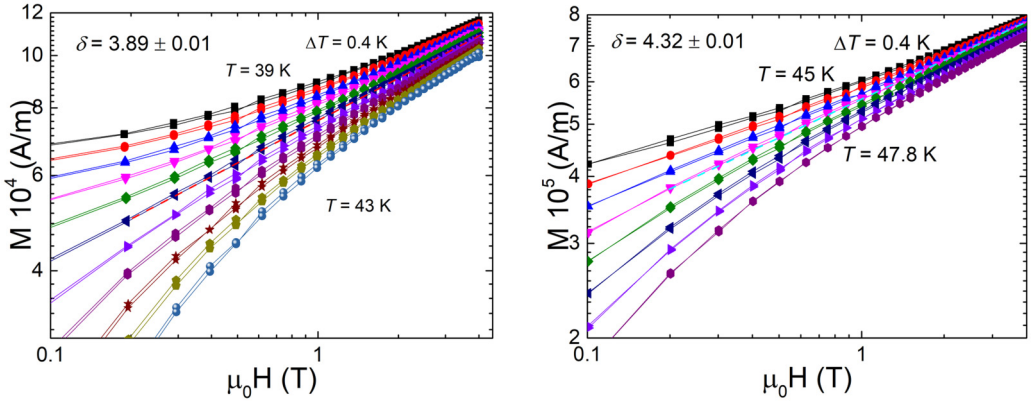

FIG. 2. Logarithmic plot of magnetic isotherms of URhGa (left) and UCoGa (right). Critical isotherms for each compound are highlighted by the dashed line. The critical exponent δ from fit to critical exponent for each compound are part of the figure.

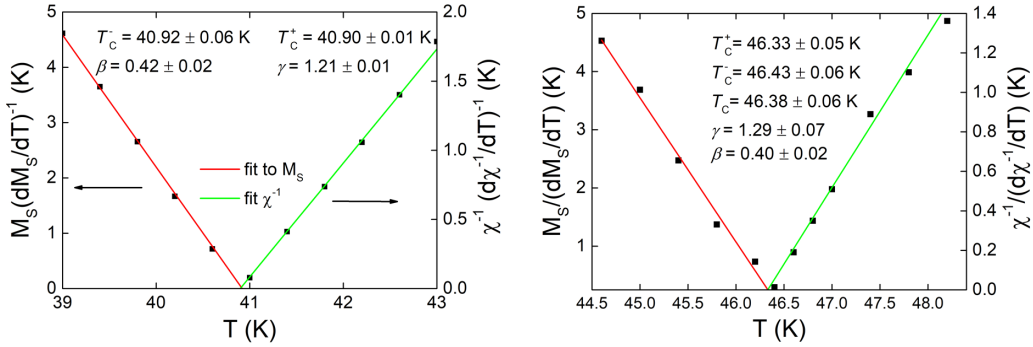

FIG. 3. Kouvel-Fisher plot for spontaneous magnetization and susceptibility for URhGa (left) and UCoGa (right). The critical exponents are shown in corresponding figures.

The critical exponents of URhGa and UCoGa can be explained similarly to the URhAl case [10] by introducing a weak long-range magnetic exchange interaction in the form $J(r) \sim r^{-(d+\sigma)}$, where σ is the range of the exchange interaction [31]. Fischer *et al.* [31] applied the renormalization group theory for a system with an interaction $J(r)$ for which the equation for γ has been obtained in the form:

$$\gamma = 1 + \frac{4}{d}\left(\frac{n+2}{n+8}\right)\Delta\sigma + \frac{8(n+2)(n-4)}{d^2(n+8)^2} \times \left[1 + \frac{2G\left(\frac{d}{2}\right)(7n+20)}{(n-4)(n+8)}\right]\Delta\sigma^2, \quad (9)$$

where $\Delta\sigma = (\sigma - \frac{d}{2})$ and $G(\frac{d}{2}) = 3 - \frac{1}{4}(\frac{d}{2})^2$. The value of σ ranges from $d/2$ to d. Outside of this interval, for $\sigma \geqslant d$, behavior typical for short-range interactions is expected, and for $\sigma \leqslant d/2$, behavior is described by mean-field theory. The obtained values of γ were examined using Eq. (9) by substituting the possible values of d (dimension of the system) = 1, 2, or 3 and n (dimension of the order parameter) = 1, 2, or 3 in all possible combinations and comparing the resulting values of σ for γ and β. The best agreement for both URhGa and UCoGa has been found for the 2D Ising system with long-range (LR) interactions, similar to URhAl [10]. The resulting σ value and corresponding β, γ, and δ values are listed in Table I and Fig. 5 with values for URhAl [10] and 3D Ising, 3D XY, 3D Heisenberg, 2D Ising, and mean field models.

B. $UCo_{0.98}Ru_{0.02}Al$

The critical exponents $\gamma = (1.27 \pm 0.01)$ and $\beta = (0.32 \pm 0.01)$ determined by Arrott-Noakes analysis of magnetization data collected on the $UCo_{0.98}Ru_{0.02}Al$ single crystal (see Arrott-Noakes plots in Fig. 6) with $T_C = 22.79$ K compare well to the theoretical values $\gamma = 1.241$ and $\beta = 0.325$ for the 3D Ising model [24,32].

Further, the value $\delta = (4.92 \pm 0.01)$ corresponding to the critical isotherm (see Fig. 6) is close to the value of 4.97 determined from Widom scaling relations using γ and β determined from Arrott-Noakes equation. The value corresponding to the critical isotherm is close to the value of 4.82 known for the 3D Ising model.

To further analyze the $UCo_{0.98}Ru_{0.02}Al$ magnetization data, the Kouvel-Fisher method (for the respective plot see Fig. 7) was used in a similar way as above. The resulting critical exponents $\gamma = (1.24 \pm 0.04)$ and $\beta = (0.33 \pm 0.01)$ with $T_C = (22.79 \pm 0.02)$ compare to values for the 3D Ising model.

We have confirmed that $UCo_{0.98}Ru_{0.02}Al$ behaves like a 3D Ising system by plotting magnetization data using the reduced equation of state in Eq. 8 with values of β and γ for the 3D Ising model in Fig. 7. The data points fall on

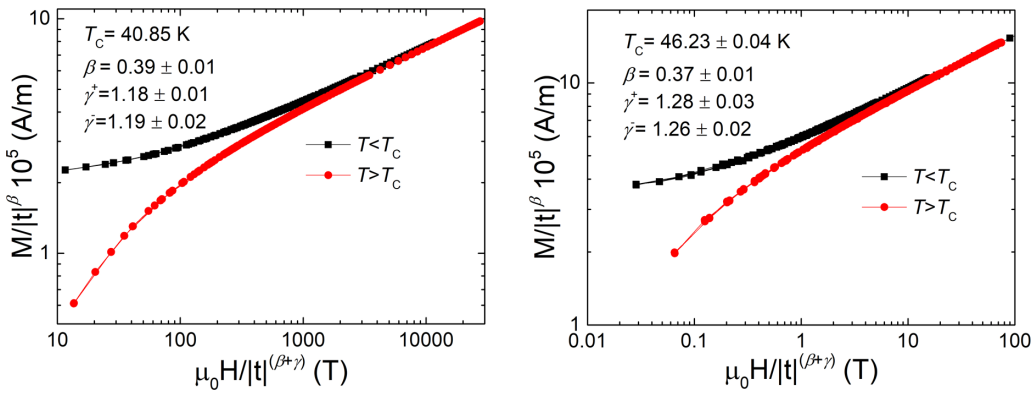

FIG. 4. The scaled magnetization plotted against the renormalized magnetic field below and above T_C. Results of fit of scaling theory from Eq. (8) for both compounds are shown in figures URhGa (left) and UCoGa (right).

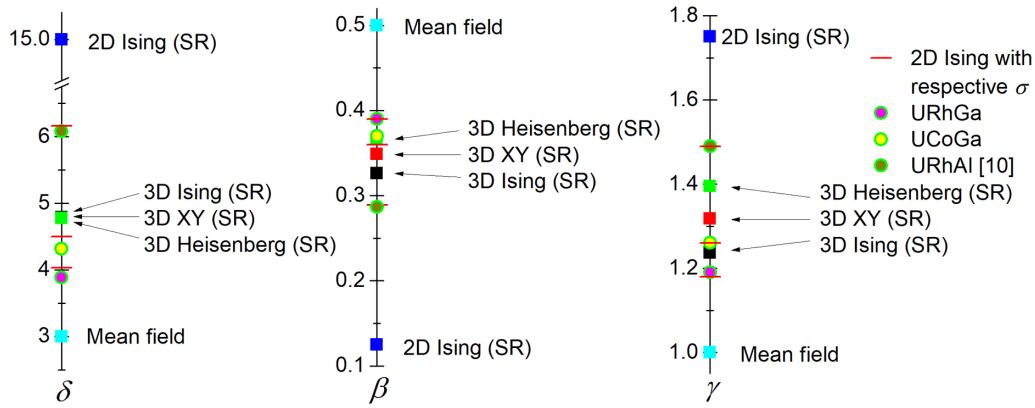

FIG. 5. Obtained critical exponents for URhGa and UCoGa in comparison to URhAl [10] and values of three-dimensional (3D) Ising, 3D XY, 3D Heisenberg, two-dimensional Ising, and mean field models.

two different curves, for T below and above $T_C = 22.74$ K, respectively, which approach asymptotically to merge. The 3D Ising behavior of $UCo_{0.98}Ru_{0.02}Al$ resembles behavior of pure UCoAl reported by Karube *et al.* [9].

The values of critical exponents and other relevant information obtained in this paper on URhGa, UCoGa, and $UCo_{0.98}Ru_{0.02}Al$ single crystals are displayed in Table I. The information available for UCoAl [9] is included for comparison and further discussion.

The table presents the most striking result of our study: although the three studied UTX ferromagnets adopt the same type of layered hexagonal crystal structure with strong uniaxial magnetocrystalline anisotropy, they do not fall in the same universality class. URhGa and UCoGa exhibit a 2D Ising character similar to URhAl [10], whereas $UCo_{0.98}Ru_{0.02}Al$ behaves as a 3D Ising system, also reported for UCoAl [9].

The $5f$-electrons in U intermetallics are known to have a dual character (partially localized, partially itinerant) [33–35]. The localized and itinerant characters appear in different proportions depending on crystallographic and chemical environments of the U ion being reflected in a wide range of their magnetic behavior. This is a consequence of the wide extension of the $5f$-wave functions which allows for considerable direct overlaps between $5f$-wave functions of the nearest-neighbor U ions as well as hybridization of valence electron states of ligands ($5f$-ligand hybridization). As a result, the original atomic character of the $5f$-wave functions is destroyed while the related magnetic moments are washed out and adequately reduced. In the strong $5f$-$5f$ overlap and $5f$-ligand hybridization limits, the $5f$-electrons are predominantly itinerant, the $5f$ magnetic moments vanish, and the magnetic order is lost (UCoAl in our case).

Rhodes and Wohlfarth [36] and Wohlfarth [37] proposed that the ratio $\mu_{\rm eff}/\mu_s$ between the effective and spontaneous magnetic moments can be taken as a measure of the degree of itinerancy of the magnetic electrons. In Table II, we can see that $\mu_{\rm eff}/\mu_s$ increases along the series as listed from top to bottom. In the Rhodes-Wohlfarth scenario, the degree of itinerancy of $5f$ electrons increases when proceeding from URhGa toward UCoAl.

We can also see that the lattice parameter a shown in the same table simultaneously decreases along the series. The close packing of U and T atoms in the basal plane of the hexagonal ZrNiAl-type structure results both in a nonnegligible $5f$-$5f$ overlap and a strong $5f$-d hybridization involving the transition metal d states which compress most of the $5f$ charge density toward the basal plane. The reduction of a is intimately connected with the decreasing U-U and U-T interatomic distances within the basal plane. The simultaneously enhanced $5f$-$5f$ overlaps and $5f$-d hybridization causes a

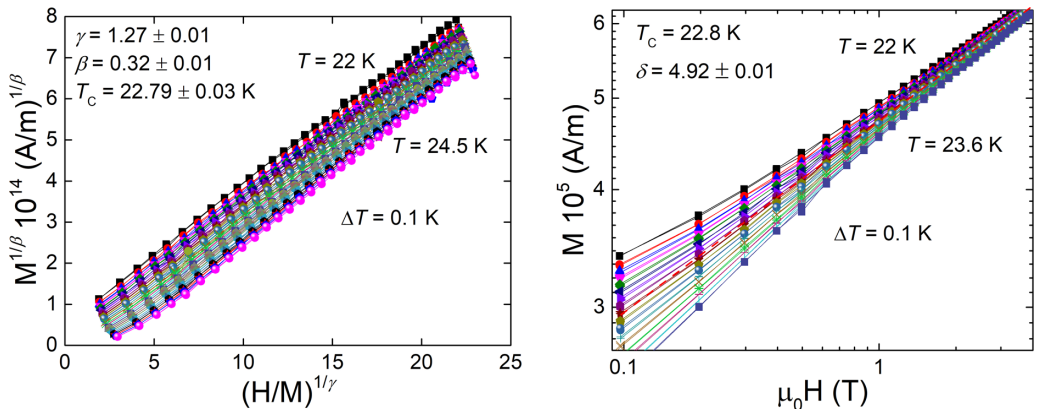

FIG. 6. Arrott-Noakes plots (left) and logarithmic plots (right) of magnetization isotherms for $UCo_{0.98}Ru_{0.02}Al$. The results of the fit by Arrott-Noakes equation [Eq. (5)] are displayed in the left figure, while in the right figure, the result of the fit by critical isotherm can be found.

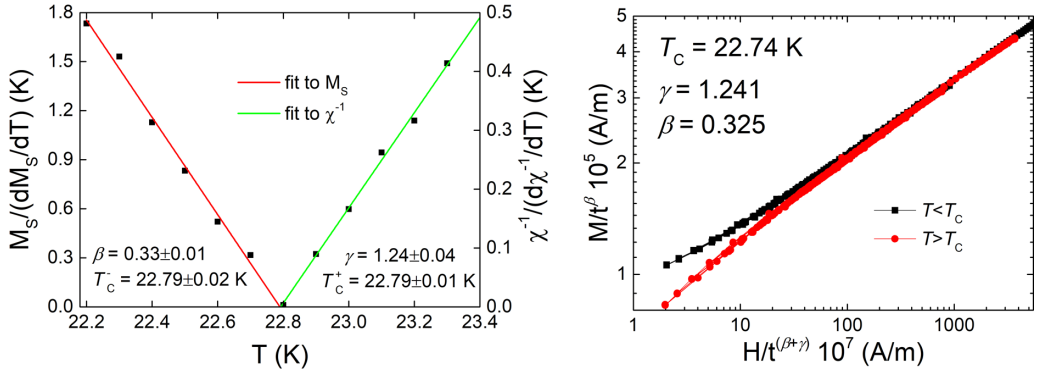

FIG. 7. Kouvel-Fisher plot of $UCo_{0.98}Ru_{0.02}Al$ with results of fit of Eqs. (6) and (7) (left). Plot of the scaled magnetization vs the rescaled magnetic field for $UCo_{0.98}Ru_{0.02}Al$ (right). Results of fit of scaling theory from Eq. (8) are part of the figure.

higher degree of itinerancy, which corroborates the Rhodes-Wohlfarth scenario.

The change from 2D to 3D behavior was described by Takahashi [38], who considers quasi-itinerant ferromagnets. In a quasi-2D system, the spin fluctuation in the z direction differs from spin fluctuations in the xy plane, which comes from the uniaxial magnetocrystalline anisotropy of the system. The critical behavior of the system in the region of the T-H space centered on [T_C, 0] is described as 3D, while outside of this region, the critical behavior is 2D. For stronger anisotropy, the region of 3D behavior is reduced. The large magnetocrystalline anisotropy observed in UTX compounds crystallizing in the ZrNiAl-type structure [8,11,15,39] leads to suppression of a 3D behavior, and instead, a 2D behavior is observed as seen in URhGa, UCoGa, and URhAl. It is important to emphasize that the systems described by Takahashi [38] show different critical behaviors, but the effect of anisotropy on the nature of fluctuations near T_C is expected to be similar.

Further inspection of Table II reveals that the change from 2D Ising to 3D Ising universality class happens when the $5f$ electrons become considerably itinerant. This agrees with Takahashi's [38] description, in which for more itinerant systems, larger anisotropy is needed to suppress the region of 3D behavior than more localized systems. This explains the 3D behavior of UCoAl and $UCo_{0.98}Ru_{0.02}Al$ even though the magnetocrystalline anisotropy is comparable to that in URhGa, UCoGa, and URhAl [8,11,15,39]. Also, we see that the p-metal affects the degree of localization/itineracy, which in turn affects the universality class of the system. The hierarchy of exchange interactions will undoubtedly play an essential role in controlling dimensionality. The involvement of theorists in resolving these issues is needed. It would also be interesting to investigate the evolution of critical exponents and magnetic dimensionality together with the development of lattice parameters while applying hydrostatic pressure. A possible change of magnetic dimensionality with applied pressure near a quantum critical point may open new questions in quantum criticality research.

IV. CONCLUSIONS

The magnetization isotherms of URhGa, UCoGa, and $UCo_{0.98}Ru_{0.02}Al$ were measured at temperatures near their ferromagnetic transitions, where we investigated the critical behavior. The values of critical exponents β, γ, and δ have been determined by analyzing magnetization data presented in Arrott-Noakes plots, Kouvel-Fisher plots, critical isotherms, scaling theory, and Widom scaling relations. The results point to the 2D Ising universality class for URhGa and UCoGa, similar to URhAl reported by other investigators [10]. Data obtained for $UCo_{0.98}Ru_{0.02}Al$ are characteristic of the 3D Ising universality class, which was suggested in previous studies also for the itinerant $5f$-electron paramagnet UCoAl. At the high degree of itinerancy of $5f$ electrons, a change from the 2D to the 3D character is observed between UCoGa and $UCo_{0.98}Ru_{0.02}Al$. Possible new phenomena may be expected when a dimensionality change happens in the vicinity of the quantum critical point.

TABLE II. The values of effective and spontaneous magnetic moment, μ_{eff} and μ_s, respectively, and the μ_{eff}/μ_s ratio and lattice parameters for our studied URhGa, UCoGa, and $UCo_{0.98}Ru_{0.02}Al$ compounds completed by the values for URhAl and UCoAl. The μ_s value for UCoAl is the magnetic moment in the field just above the metamagnetic transition. The true μ_s value for UCoAl is indeed equal to 0; the ground state is paramagnetic.

Compound	μ_{eff}(μ_B/f.u.)	μ_s(μ_B/f.u.)	μ_{eff}/μ_s	Ref.	Universality class	a (pm)	c (pm)	Ref.
URhGa	2.45	1.17	2.11	[40]	2D Ising	700.6	394.5	[41]
URhAl	2.50	1.05	2.38	[10]	2D Ising	696.5	401.9	[41]
UCoGa	2.40	0.65	3.69	[15]	2D Ising	669.3	393.3	[41]
$UCo_{0.98}Ru_{0.02}Al$	1.73	0.36	4.81	[a]	3D Ising	669.1	396.6	[a]
UCoAl	1.60	0.30	5.33	[11]	3D Ising	668.6	396.6	[42]

[a]Unpublished data.

ACKNOWLEDGMENTS

This research was supported by Grant Agency of Charles University (Grant No. 1630218) and by the Czech Science Foundation (Grant No. 16-06422S). Experiments were performed in MGML [43], which is supported within the program of Czech Research Infrastructures (Project No. LM2018096). It was also supported by OP VVV project MATFUN under Grant CZ.02.1.01/0.0/0.0/15_003/0000487. We would also like to thank Dr. Ross Colman for proofreading of the text and language corrections.

[1] T. Andrews, XVIII. *The Bakerian Lecture*.—On the continuity of the gaseous and liquid states of matter, Philos. Trans. R. Soc. London **159**, 575 (1869).

[2] J. Hopkinson, I. Magnetic properties of alloys of nickel and iron, Proc. R. Soc. London **48**, 1 (1891).

[3] M. E. Fisher, The theory of equilibrium critical phenomena, Reports Prog. Phys. **30**, 615 (1967).

[4] L. P. Kadanoff, Scaling laws for Ising models near T_C, Phys. Phys. Fiz. **2**, 263 (1966).

[5] K. G. Wilson, Renormalization group and critical phenomena. I. Renormalization group and the Kadanoff scaling picture, Phys. Rev. B **4**, 3174 (1971).

[6] K. G. Wilson, Renormalization group and critical phenomena. II. Phase-space cell analysis of critical behavior, Phys. Rev. B **4**, 3184 (1971).

[7] K. G. Wilson, The renormalization group: Critical phenomena and the Kondo problem, Rev. Mod. Phys. **47**, 773 (1975).

[8] V. Sechovsky and L. Havela, Chapter 1. Magnetism of ternary intermetallic compounds of uranium, in *Handbook of Magnetic Materials*, edited by K. H. J. Buschow (Elsevier, Amsterdam, 1998), Vol. 11, Chap. 1, pp. 1–289.

[9] K. Karube, T. Hattori, S. Kitagawa, K. Ishida, N. Kimura, and T. Komatsubara, Universality and critical behavior at the critical endpoint in the itinerant-electron metamagnet UCoAl, Phys. Rev. B **86**, 024428 (2012).

[10] N. Tateiwa, J. Pospíšil, Y. Haga, and E. Yamamoto, Critical behavior of magnetization in URhAl: Quasi-two-dimensional Ising system with long-range interactions, Phys. Rev. B **97**, 064423 (2018).

[11] V. Sechovsky, L. Havela, F. R. de Boer, J. J. M. Franse, P. A. Veenhuizen, J. Sebek, J. Stehno, and A. V. Andreev, Systematics across the U*TX* Series (T = Ru, Co, Ni; X = Al, Ga, Sn) of high-field and low-temperature properties of non-ferromagnetic compounds, Physica B+C **142**, 283 (1986).

[12] N. Tateiwa, J. Pospíšil, Y. Haga, H. Sakai, T. D. Matsuda, and E. Yamamoto, Itinerant ferromagnetism in actinide $5f$-electron systems: Phenomenological analysis with spin fluctuation theory, Phys. Rev. B **96**, 035125 (2017).

[13] A. V. Andreev, A. V. Deryagin, and R. Y. Yumaguzhin, Crystal structure and magnetic properties of UGaCo and UGaNi single crystals, Sov. Phys. JETP **59**, 1082 (1984).

[14] P. Opletal, P. Proschek, B. Vondráčková, D. Aurélio, V. Sechovský, and J. Prokleška, Effect of thermal history on magnetism in UCoGa, J. Magn. Magn. Mater. **490**, 165464 (2019).

[15] H. Nakotte, F. R. de Boer, L. Havela, P. Svoboda, V. Sechovsky, Y. Kergadallan, J. C. Spirlet, and J. Rebizant, Magnetic anisotropy of UCoGa, J. Appl. Phys. **73**, 6554 (1993).

[16] V. Sechovsky, F. Honda, K. Prokes, O. Syshchenko, A. V. Andreev, and J. Kamarad, Pressure-induced phenomena in U intermetallics, Acta Phys. Pol. B **34**, 1377 (2003).

[17] V. Sechovský, L. Havela, N. Pillmayr, G. Hilscher, and A. V. Andreev, On the magnetic behaviour of UGaT series, J. Magn. Magn. Mater. **63–64**, 199 (1987).

[18] V. Sechovsky, L. Havela, F. R. de Boer, P. A. Veenhuizen, K. Sugiyama, T. Kuroda, E. Sugiura, M. Ono, M. Date, and A. Yamagishi, Hybridization and magnetism in U(Ru, Rh)X, X = Al, Ga, Phys. B Condens. Matter **177**, 164 (1992).

[19] A. V. Andreev, L. Havela, V. Sechovsky, M. I. Bartashevich, J. Sebek, R. V. Dremov, and I. K. Kozlovskaya, Ferromagnetism in the $UCo_{1-x}Ru_xAl$ quasiternary intermetallics, Philos. Mag. B **75**, 827 (1997).

[20] P. Opletal, J. Prokleška, J. Valenta, P. Proschek, V. Tkáč, R. Tarasenko, M. Běhounková, Š. Matoušková, M. M. Abd-Elmeguid, and V. Sechovský, Quantum ferromagnet in the proximity of the tricritical point, npj Quantum Mater. **2**, 29 (2017).

[21] A. Arrott, Criterion for ferromagnetism from observations of magnetic isotherms, Phys. Rev. **108**, 1394 (1957).

[22] A. Arrott and J. E. Noakes, Approximate Equation of State for Nickel Near its Critical Temperature, Phys. Rev. Lett. **19**, 786 (1967).

[23] J. S. Kouvel and M. E. Fisher, Detailed magnetic behavior of nickel near its Curie point, Phys. Rev. **136**, A1626 (1964).

[24] V. Privman, P. C. Hohenberg, and A. Aharony, Universal critical-point amplitude relations, in *Phase Transitions and Critical Phenomena*, edited by C. Domb and J. L. Lebowitz (Academic Press Limited, London, 1991), Vol. 14, p. 367.

[25] B. Widom, Equation of state in the neighborhood of the critical point, J. Chem. Phys. **43**, 3898 (1965).

[26] A. Aharoni, Demagnetizing factors for rectangular ferromagnetic prisms, J. Appl. Phys. **83**, 3432 (1998).

[27] L. D. Landau, On the theory of phase transitions. I., Zh. Eksp. Teor. Fiz. **7**, 19 (1937).

[28] L. D. Landau, On the theory of phase transitions. I., Phys. Z. Sowjet. **11**, 26 (1937).

[29] D. Ter Haar, On the theory of phase transitions, *Men of Physics: L.D. Landau* (Elsevier, Oxford, 1969), pp. 61–84.

[30] V. L. Ginzburg, Behavior of ferromagnetic substances in the vicinity of the Curie point, Zh. Eksp. Teor. Fiz. **17**, 833 (1947).

[31] M. E. Fisher, S. K. Ma, and B. G. Nickel, Critical Exponents for Long-Range Interactions, Phys. Rev. Lett. **29**, 917 (1972).

[32] J. C. Le Guillou and J. Zinn-Justin, Critical exponents from field theory, Phys. Rev. B **21**, 3976 (1980).

[33] T. Takahashi, N. Sato, T. Yokoya, A. Chainani, T. Morimoto, and T. Komatsubara, Dual character of $5f$ electrons in UPd_2Al_3 observed by high-resolution photoemission spectroscopy, J. Phys. Soc. Japan **65**, 156 (1996).

[34] G. Zwicknagl, $5f$ electron correlations and core level photoelectron spectra of uranium compounds, Phys. Status Solidi **250**, 634 (2013).

[35] G. Zwicknagl, $3 = 2 + 1$: partial localization, the dual character of $5f$ electrons and heavy fermions in U compounds, J. Magn. Magn. Mater. **272–276**, E119 (2004).

[36] P. Rhodes and E. P. Wohlfarth, The effective Curie-Weiss constant of ferromagnetic metals and alloys, Proc. R. Soc. Lond. A. **273**, 247 (1963).

[37] E. P. Wohlfarth, Magnetic properties of crystalline and amorphous alloys: A systematic discussion based on the Rhodes-Wohlfarth plot, J. Magn. Magn. Mater. **7**, 113 (1978).

[38] Y. Takahashi, Spin-fluctuation theory of quasi-two-dimensional itinerant-electron ferromagnets, J. Phys. Condens. Matter **9**, 10359 (1997).

[39] P. A. Veenhuizen, F. R. de Boer, A. A. Menovsky, V. Sechovsky, and L. Havela, Magnetic-properties of URuAl and URhAl single-crystals, J. Phys. **49**, 485 (1988).

[40] P. Opletal, Peculiarities of magnetism on the verge of ferromagnetic ordering, Ph.D. thesis, Charles University, 2019.

[41] A. E. Dwight, Alloy chemistry of thorium, uranium, and plutonium compounds, in *Developments in the Structural Chemistry of Alloy Phases*, edited by B. C. Giessen (Springer, Boston, 1969), pp. 181–226.

[42] D. J. Lam, J. B. Darby, J. W. Downey, and L. J. Norton, Equiatomic ternary compounds of uranium and aluminium with Group VIII transition elements, J. Nucl. Mater. **22**, 22 (1967).

[43] www.mgml.eu.